

Supporting Information

A breathable and reliable thermoplastic polyurethane/Ag@K₂Ti₄O₉, composite film with asymmetrical porous structure for wearable piezoresistive sensors

Ziwei Chen,^{a†} Mingxu Wang,^{b†} Chenyang Zhang,^a Zhongrui Wei,^a Yuhang Wang,^a
Chunxia Gao,^{a*} Jiadeng Zhu,^{c*} Jiefeng Gao,^a Ming Shen,^a and Qiang Gao^{a*}

*^aSchool of Chemistry and Chemical Engineering, Yangzhou University, Yangzhou,
225002, China*

*^bGraduate School of Medicine, Science and Technology, Shinshu University, 3-15-1,
Tokida, Ueda, Nagano, 386-8567 Japan*

*^cChemical Sciences Division, Oak Ridge National Laboratory, Oak Ridge, TN 37831,
USA*

Corresponding author: Dr. Qiang Gao (gaoqiang@yzu.edu.cn), Dr. Jiadeng Zhu
(zhujiadeng@gmail.com) or Dr. Chunxia Gao (cxgao@yzu.edu.cn)

[†]These authors contributed equally to this work.

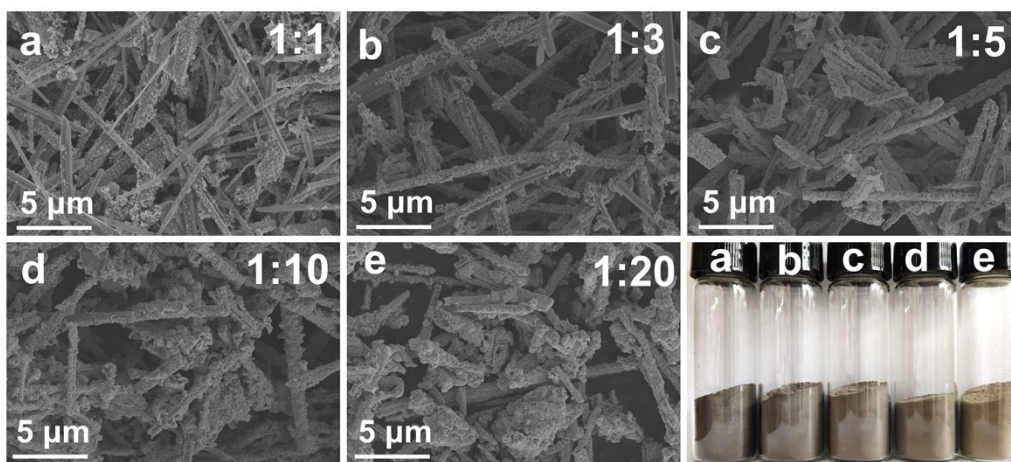


Fig. S1 SEM images of AKT whiskers with different amounts of silver nitrate per gram of potassium tetratitanate whiskers: (a) 1:1, (b) 1:3, (c) 1:5, (d) 1:10, (e) 1:20, and their corresponding digital images.

Ag particles were gradually formed on the surface of whiskers to generate conductive paths.

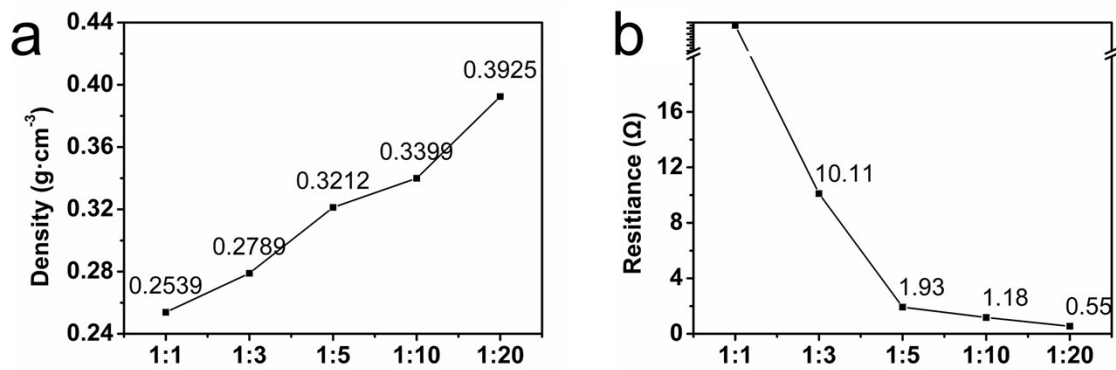


Fig. S2 The relationship of (a) density and (b) resistance of AKT whiskers with different amounts of silver nitrate per gram of potassium tetratitanate whiskers.

The resistance of the whisker was measured by the following method: put 0.05 g of AKT whiskers into a circular container with a diameter of 1 cm, and measure the resistance at both ends of the diameter.

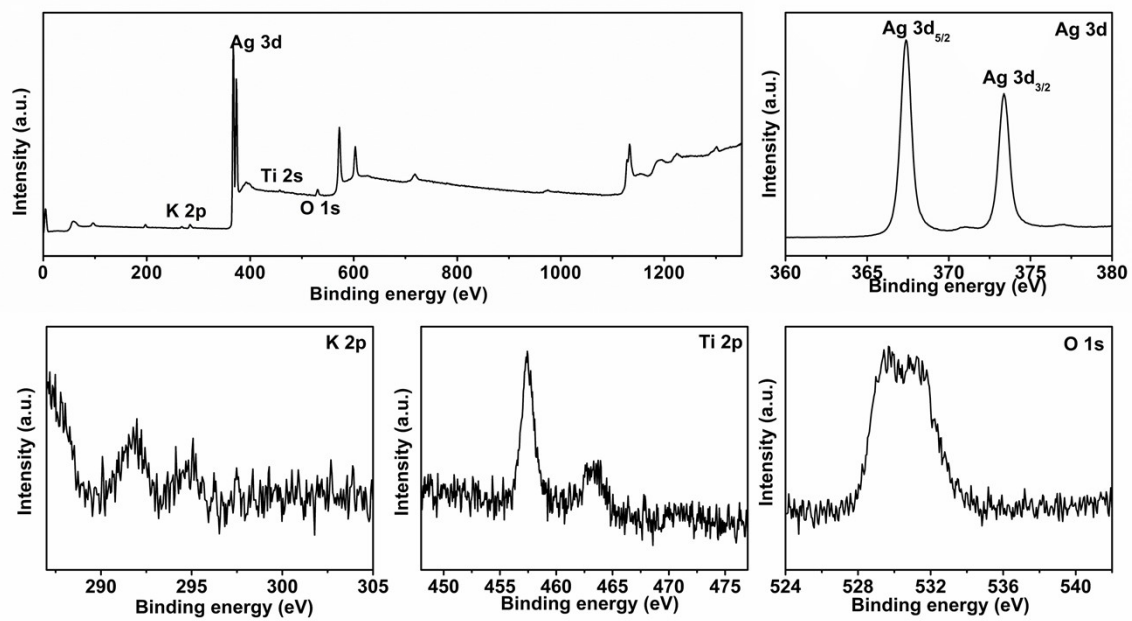


Fig. S3 XPS spectra of different elements of $K_2Ti_4O_9$.

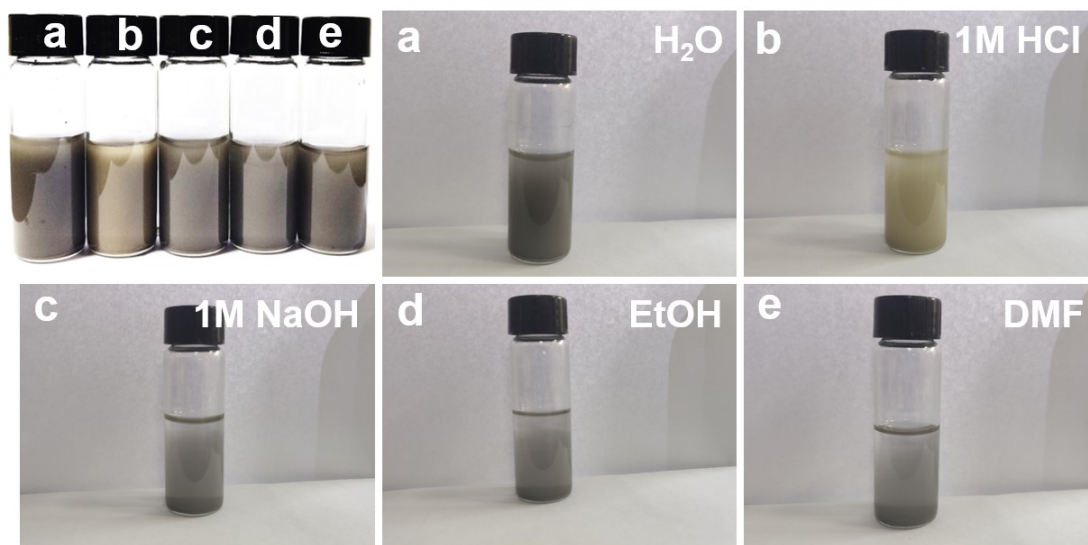


Fig. S4 Dispersion of whiskers in different solvents/solutions after 10 min: (a) H₂O, (b) 1 M HCl, (c) 1 M NaOH, (d) EtOH, and (e) DMF.

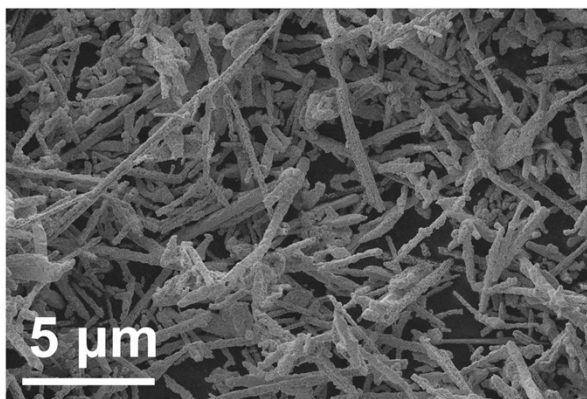


Fig. S5 An SEM image of the AKT power stored in the glass bottle for more than 180 days under dark conditions.

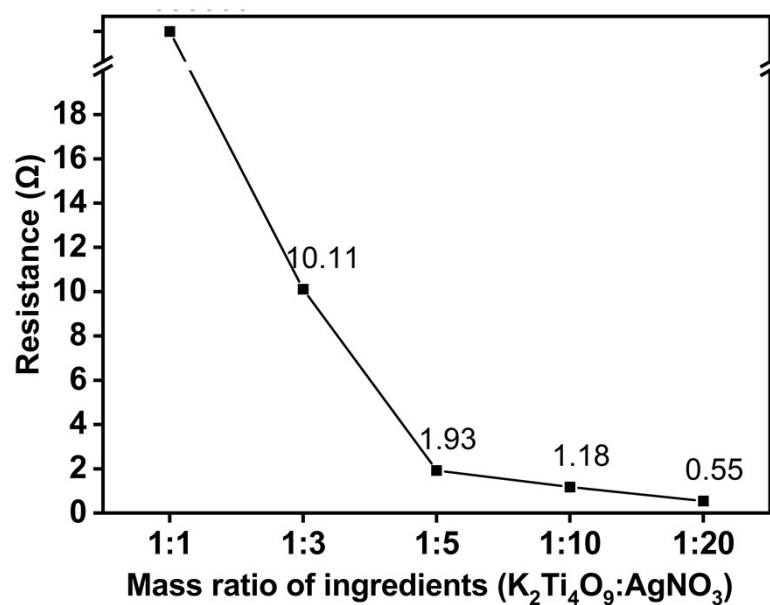


Fig. S6 Conductivity of AKT powers prepared by using different mass ratios of ingredients (K₂Ti₄O₉:AgNO₃) stored in glass bottles for more than 180 days under dark conditions.

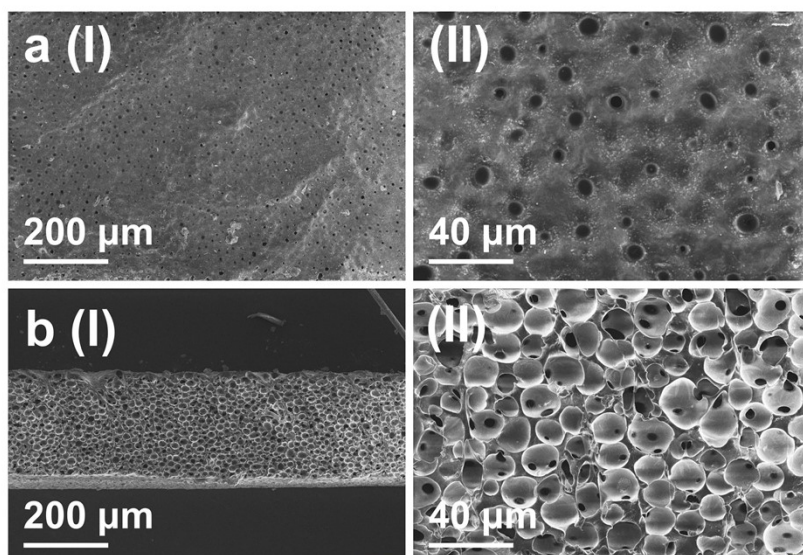


Fig. S7 (a) Surface and (b) sectional SEM images of the pure TPU membrane prepared by NIPS.

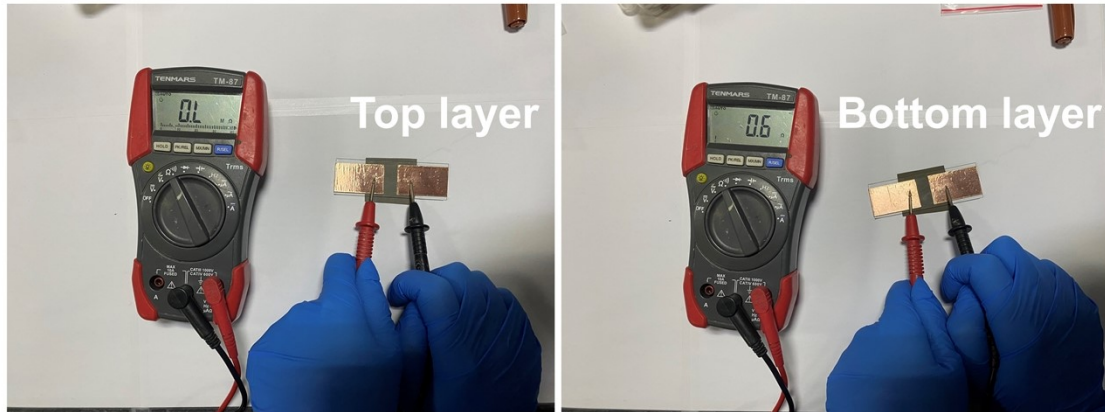


Fig. S8 The contact resistance of the top (a) and bottom (b) layers.

We stucked conductive copper tape on both sides of the glass sheet (The two edges were joined), and left 1 cm in the middle. This is a simple way to measure the surface contact resistance. The surface resistance of the top layer is out of range (O.L.>100 M Ω), and the surface resistance of the bottom layer is 0.6 Ω .

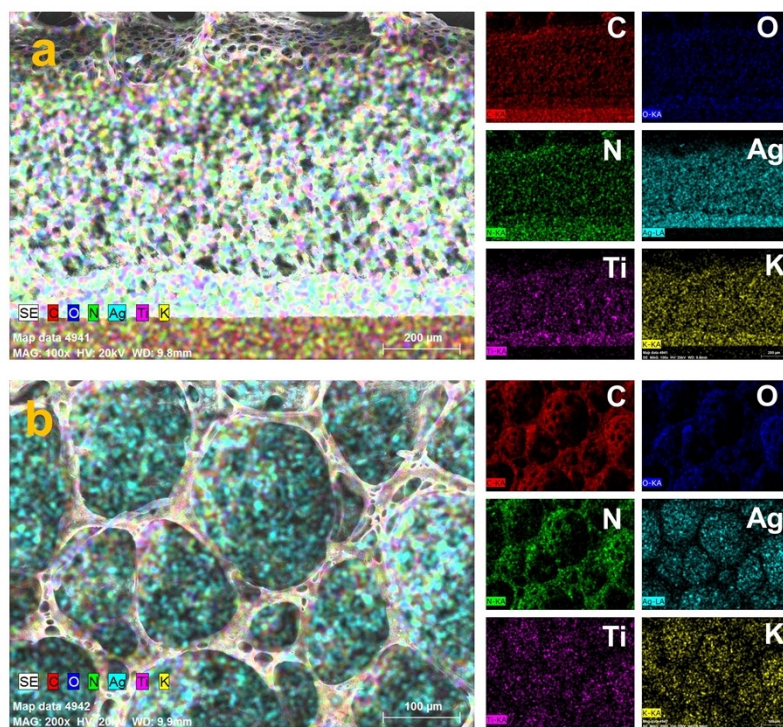


Fig. S9 EDS mapping images of the sectional (a) and top (b) layers of the hierarchical porous TPU/AKT hybrid membrane.

As can be seen from **Fig. S9a**, the Ag content in the bottle layer is much higher than that in the top layer, but the amount of silver element in the intermediate porous layer is uniform. **Fig. S9b** shows that the top layer of macro-porous framework contains less silver.

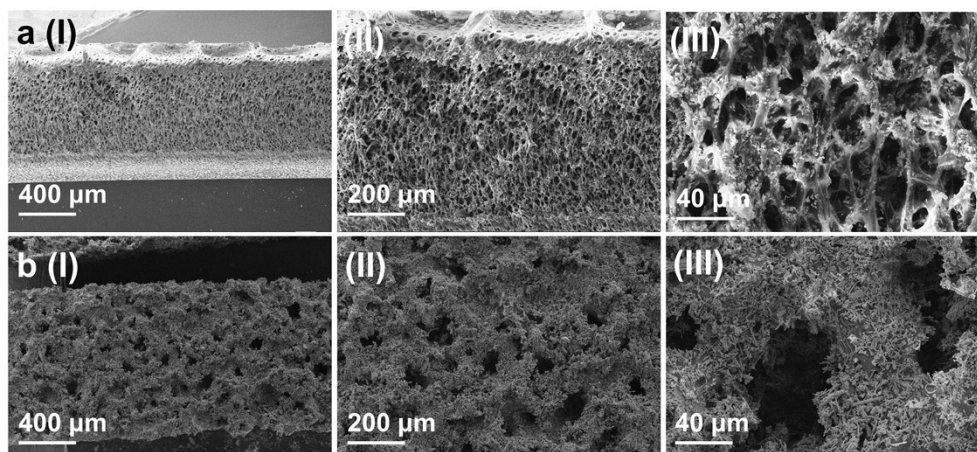


Fig. S10 Sectional SEM images of the porous TPU/AKT hybrid membranes prepared at (a) 25°C and (b) 50°C.

The electron microscopy well demonstrates our proposed mechanism. (**Fig. S10a**) At the appropriate temperature, the mixed liquid with only TPU floating through the network to form the top layer. The holes in the section are elongated vertically, which can be interpreted as the result of upward movement of the mixed liquid with TPU. (**Fig. S10b**) Network-distributed whiskers **cannot** provide additional anchoring effect to aggregate TPU molecular chain together to fix itself because of a relatively high temperature. Thus, a symmetrical porous membrane is formed, and the whiskers float on the surface of the TPU, showing a completely different state from the products prepared at a low temperature.

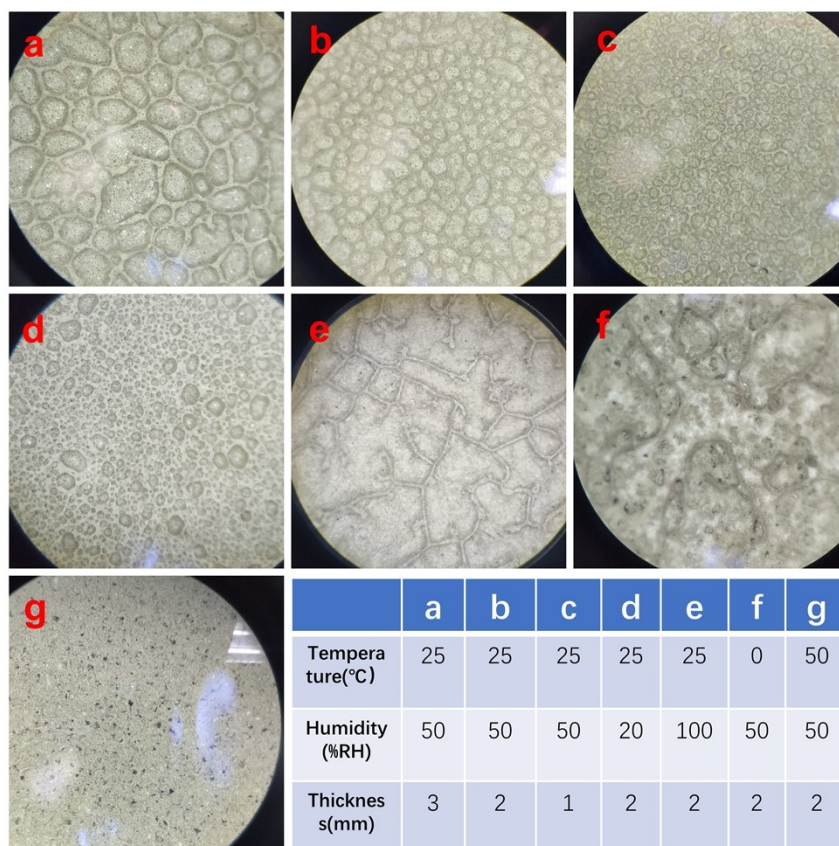


Fig. S11 Microscopic photographs of the films (top layer) prepared under different conditions.

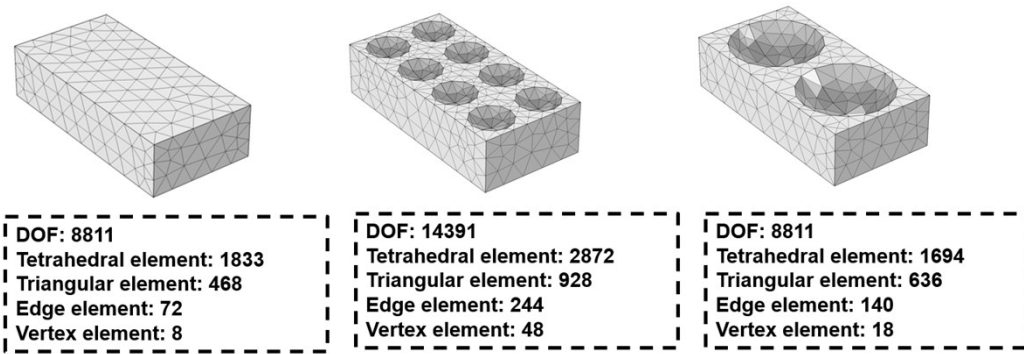
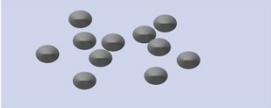

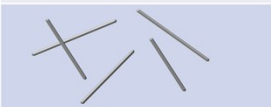




Fig. S12 The specific grid division of three representative examples (without pore, suitable pore and big pore)

For pressure simulation analysis, the COMSOL software platform was used to establish the porous structure analysis model. Solid mechanics is selected to perform the simulation process of the microstructure surface. For three representative examples, including without pore, suitable pore and big pore, were used for analysis. The entire model was meshed by over 2000 elements and more than 8000 degrees of freedom.

	Conductivity	Mechanical capacity
	Very low	Medium
	Low	Poor
	Low	Fine
	High	Medium
	Very high	Poor

AKT/TPU slurry =20%

Chosen

Fig. S13 Schematic images showing the effect of different conductive materials on the film, which proves that appropriate amount of conductive whisker provides a guarantee for high electrical conductivity along with good mechanical properties.

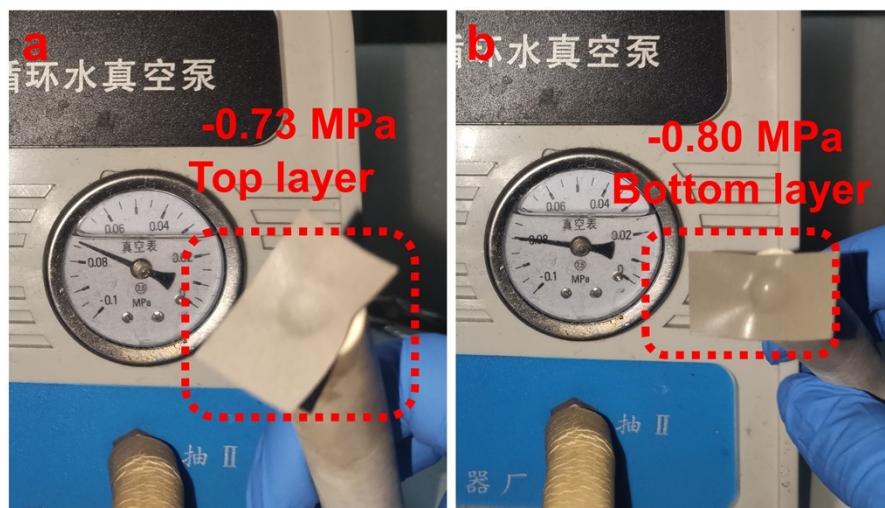


Fig. S14 Photos show that the gas passing efficiencies on the top (a) and bottom (b) layers of the membrane are different.

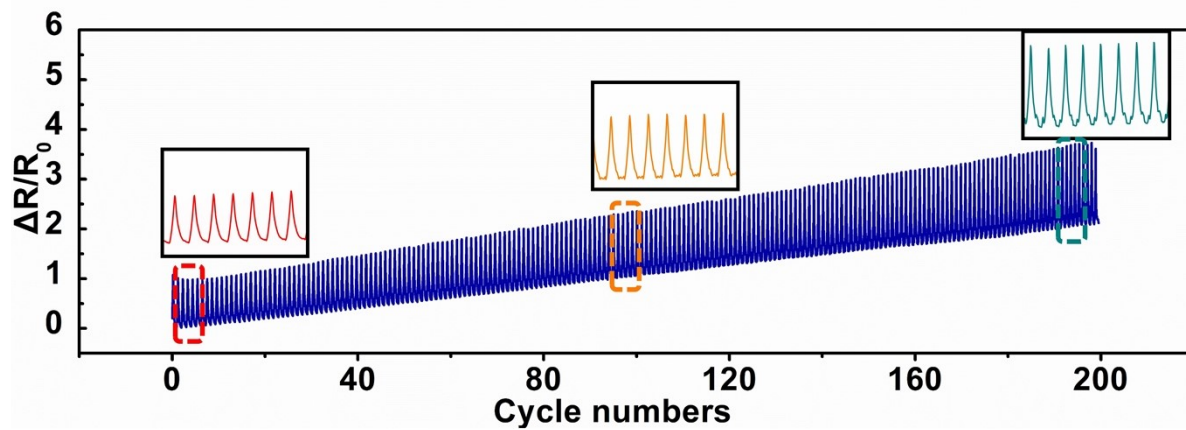


Fig. S15 The strain sensing behavior of the hierarchical porous TPU/AKT membrane during repeated stretching-relaxing deformations.

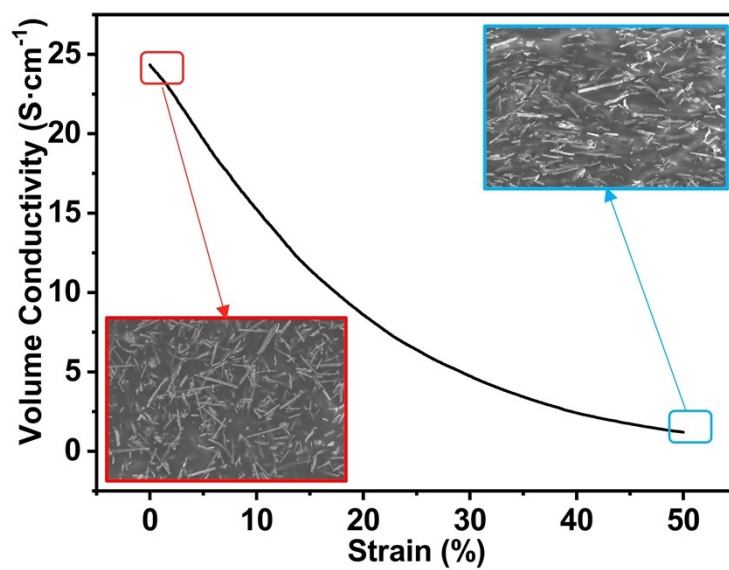


Fig. S16 The volume conductivity changes of the film while stretching.

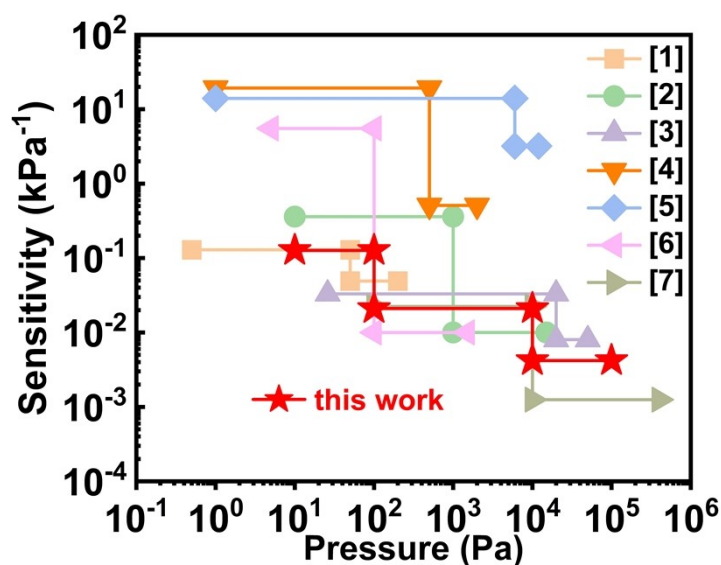


Fig. S17. Comparison with other similar works ^[1-7]

- [1] M.R. Chen, W.F. Luo, Z.Q. Xu, X.P. Zhang, B. Xie, G.H. Wang, M. Han, An ultrahigh resolution pressure sensor based on percolative metal nanoparticle arrays, *Nature Communications*, 10 (2019) 1-9.
- [2] J.Y. Yang, Y.S. Ye, X.P. Li, X.Z. Lu, R.J. Chen, Flexible, conductive, and highly pressure-sensitive graphene-polyimide foam for pressure sensor application, *Composites Science and Technology*, 164 (2018) 187-194.
- [3] Y. Song, H.T. Chen, Z.M. Su, X.X. Chen, L.M. Miao, J.X. Zhang, X.L. Cheng, H.X. Zhang, Highly Compressible Integrated Supercapacitor-Piezoresistance-Sensor System with CNT-PDMS Sponge for Health Monitoring, *Small*, 13 (2017) 1702091.
- [4] C.F. Yang, L.L. Li, J.X. Zhao, J.J. Wang, J.X. Xie, Y.P. Cao, M.Q. Xue, C.H. Lu, Highly Sensitive Wearable Pressure Sensors Based on Three-Scale Nested Wrinkling Microstructures of Polypyrrole Films, *ACS Applied Materials & Interfaces*, 10 (2018) 25811-25818.
- [5] G.Y. Bae, S.W. Pak, D. Kim, G. Lee, D. Kim, Y. Chung, K. Cho, Linearly and Highly Pressure-Sensitive Electronic Skin Based on a Bioinspired Hierarchical Structural Array, *Advanced Materials*, 28 (2016) 5300-5306.
- [6] B.W. Zhu, Z.Q. Niu, H. Wang, W.R. Leow, H. Wang, Y.G. Li, L.Y. Zheng, J. Wei, F.W. Huo, X.D. Chen, Microstructured Graphene Arrays for Highly Sensitive Flexible Tactile Sensors, *Small*, 10 (2014) 3625-3631.
- [7] Q.L. Hua, J.L. Sun, H.T. Liu, R.R. Bao, R.M. Yu, J.Y. Zhai, C.F. Pan, Z.L. Wang, Skin-inspired highly stretchable and conformable matrix networks for multifunctional sensing, *Nature Communications*, 9 (2018) 1-11.